Winds of Stars and Exoplanets
Proceedings IAU Symposium No. 370, 2023
A. A. Vidotto, L. Fossati & J. S. Vink, eds.
doi:10.1017/S1743921322004963

Effect of stellar flares and coronal mass ejections on the atmospheric escape from hot Jupiters

Gopal Hazra[1], Aline A. Vidotto[2], Stephen Carolan[3], Carolina Villarreal D'Angelo[4] and Ward Manchester[5]

[1]Dept. of Astrophysics, University of Vienna, Türkenschanzstrasse 17, A-1180 Vienna, Austria

[2]Leiden Observatory, Leiden University, NL-2300 RA Leiden, the Netherlands

[3]School of Physics, Trinity College Dublin, Dublin 2, Ireland

[4]Instituto de Astronomía Teórica y Experimental (IATE-CONICET). Laprida 854, Córdoba, Argentina

[5]Department of Climate and Space Sciences and Engineering, University of Michigan, Ann Arbor, MI 48109, USA

Abstract. Spectral observations in the Ly-α line have shown that atmospheric escape is variable and for the exoplanet HD189733b, the atmospheric evaporation goes from undetected to enhanced evaporation in a 1.5 years interval. To understand the temporal variation in the atmospheric escape, we investigate the effect of flares, winds, and CMEs on the atmosphere of hot Jupiter HD189733b using 3D self-consistent radiation hydrodynamic simulations. We consider four cases: first, the quiescent phase including stellar wind; secondly, a flare; thirdly, a CME; and fourthly, a flare followed by a CME. We find that the flare alone increases the atmospheric escape rate by only 25%, while the CME leads to a factor of 4 increments, in comparison to the quiescent case. We also find that the flare alone cannot explain the observed high blue-shifted velocities seen in the Ly-α. The CME, however, leads to an increase in the velocity of escaping atmospheres, enhancing the blue-shifted transit depth.

Keywords. stars: activity, stars: flares, stars:wind, outflows

1. Introduction

Atmospheric escape from the hot Jupiters is well observed from various spectroscopic observations (e.g., Vidal-Madjar et al. 2003; Lecavelier des Etangs et al. 2012). The radiation from host star ionises the upper atmospheres of these planets and drives a photoionized planetary outflow (e.g., Murray-Clay et al. 2009; Hazra et al. 2020). As a result atmosphere escapes from the planet. This escaping planetary outflow further interacts with the stellar environments (e.g., stellar wind, stellar coronal mass ejections (CMEs) and stellar magnetic field). Depending upon the pressure balance between strength of the stellar wind and planetary outflow, atmospheric escape gets enhanced or confined by the stellar wind (see Carolan et al. (2021) for details). The transients events (CMEs and flares) also play a crucial role on the atmospheric escape. Generally, CMEs change the properties of stellar wind plasma and flares enhance the energy deposition in the upper atmospheres of the planet affecting the dynamics of planetary atmosphere.

The transit observations of the classic hot Jupiter HD189733b showed that the atmosphere of HD189733b is undergoing through atmospheric loss due to atmospheric escape

(Lecavelier des Etangs et al. 2012). Not only it goes through an atmospheric loss, it has a temporal variation in the atmospheric escape rate most likely due to the transients events on the host star. Two transit observations of HD189733b on two epochs using the hubble space telescope (HST) showed a temporal variation in the evaporating atmosphere. While in the first epoch of observations (April, 2010) evaporation was not detected, a transit absorption depths of $14.4\% \pm 3.6\%$ in Ly-α was observed in the second epoch (September 2011). Just 8-hours before the second transit observation, an x-ray flare was observed in the host stars supporting the idea that the atmosphere of HD189733b went through an enhancement of escape caused by a transient event of the host star (Lecavelier des Etangs et al. 2012).

In this work, we study the effect of a flare, a CME and both simultaneously on the atmospheres of HD189733b to understand how these transient events affect the atmospheric escape rate. We develop a radiation driven 3D atmospheric escape model where the photoionisation due to stellar radiation in the upper atmospheres is considered self-consistently by solving radiation hydrodynamic equations. This self-consistent model gives us a unique opportunity to study the effect of stellar radiation, stellar outflows on the atmosphere of hot Jupiters and corresponding transit signature in the Ly-α line.

2. 3D atmospheric escape model and planetary outflow

We have used the BATS-R-US code to model atmospheric escape and its interaction with the stellar wind for the star-planet system HD189733. We have developed a new module in the BATS-R-US framework to solve radiation hydrodynamic equations in the rotating frame of the planet in a 3D Cartesian box keeping the planet at the origin. In the new module, we include photoionisation, collisional ionisation and corresponding heating and cooling terms. For details of the model, see Section-2 of Hazra et al. (2022).

As the X-ray and Extreme Ultra Violet (EUV) part of stellar spectra is responsible for photoionisation, we need information about XUV radiation from the host star HD189733A. Because of not availability of EUV spectra of the star from observations currently, we calculate that part of the spectra from empirical relation given in equation (3) of Sanz-Forcada et al. (2011) from measured X-ray luminosity in the quiescent phase of the star. The estimated value of XUV (X-ray and EUV) luminosity during the queiscent phase of the star is $L_{\rm xuv} = 1.3 \times 10^{29}$ erg s^{-1}. Although, our model is capable of incorporating multi-species, we assume a hydrogen dominated atmosphere for simplicity.

We show the basic features of planetary outflow due to self-consistent deposition of stellar radiation from our escape model in figure 1. In the figure 1(a), the total density of outflowing planetary materials is shown in the orbital plane. As it is clear from the figure that the planetary material moves in a clockwise direction after it is able to escape from the planetary gravity due to the Coriolis force. The velocity streamlines are shown in black contours. The neutral density is shown in figure 1(b). For tidally locked planet, the night side does not receive enough stellar radiation and the night side material is no longer ionised leading to the formation of a planetary tail of neutral material as seen in figure 1(b).

Figure 1(c) and figure 1(d) show the temperature and velocity of the planetary materials. A shock is formed when the oppositely deflected material meets due to interplay between tidal force and Coriolis force, which is found in the high temperature region i.e., the tangential between quadrants I and IV and quadrants II and III in figure 1(c).The sonic surface is shown in black contour in figure 1(d). All of these basic features of planetary outflow are very consistent with previous studies (e.g., McCann et al. 2019). The atmospheric escape rate from the planet is 6.0×10^{10} g s^{-1}, which is consistent with previous models (Salz et al. 2016, and reference therein) in spite of the different implementation of various physical processes.

https://doi.org/10.1017/S1743921322004963 Published online by Cambridge University Press

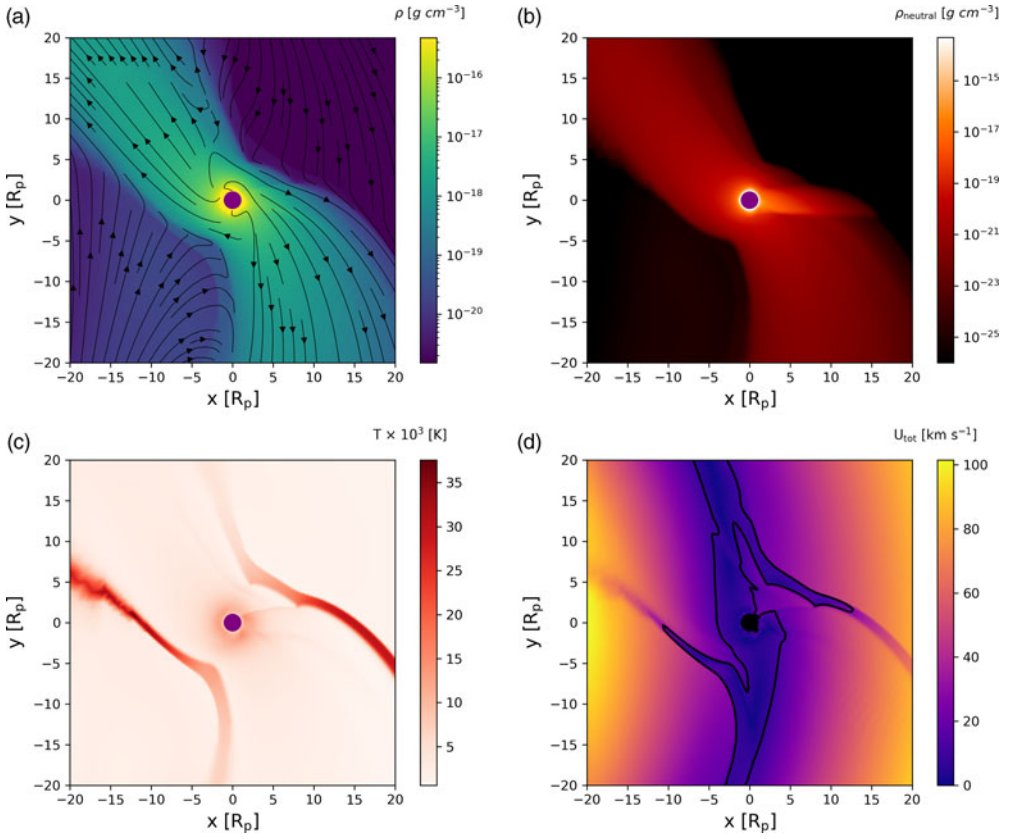

Figure 1. Basic features of planetary outflow. (a) Total density with velocity streamlines, (b) neutral density, (c) temperature distribution and (d) Total velocity with sonic surface in black contour. All plots are in the orbital plane.

3. Effect of stellar transient events on the planetary atmosphere

To study the effect of flares and CMEs on the atmospheres of the hot Jupiter HD189733b, we consider three instances of transient events. In first instance, we consider only a flare, then we consider a CME and finally we consider the effect of a flare associated with a CME. As we mentioned earlier, flares enhance the stellar radiation and CME changes the stellar wind plasma density. Hence we change stellar radiation and stellar wind parameters according to the case we study. We consider four cases to capture the full stellar environments as given below.

3.1. *Case-I: quiescent phase*

In the quiescent phase of the star, we consider the XUV radiation at quiet phase and the background stellar wind. The stellar wind in this case interacts with the XUV driven planetary outflow as presented in Section 2. In our model, stellar wind is modelled as a 1D isothermal Parker wind and injected from the negative x boundary of our simulation box. The properties of the stellar wind temperature and mass-loss rate is taken from stellar wind simulation of K dwarf HD189733A (Kavanagh et al. 2019). The final properties of planetary outflow is depicted in the first column of the figure 2. The total density, neutral density, temperature and total velocity are shown from top to bottom rows of figure 2 respectively in the first column. The black contours in the top row show the velocity

https://doi.org/10.1017/S1743921322004963 Published online by Cambridge University Press

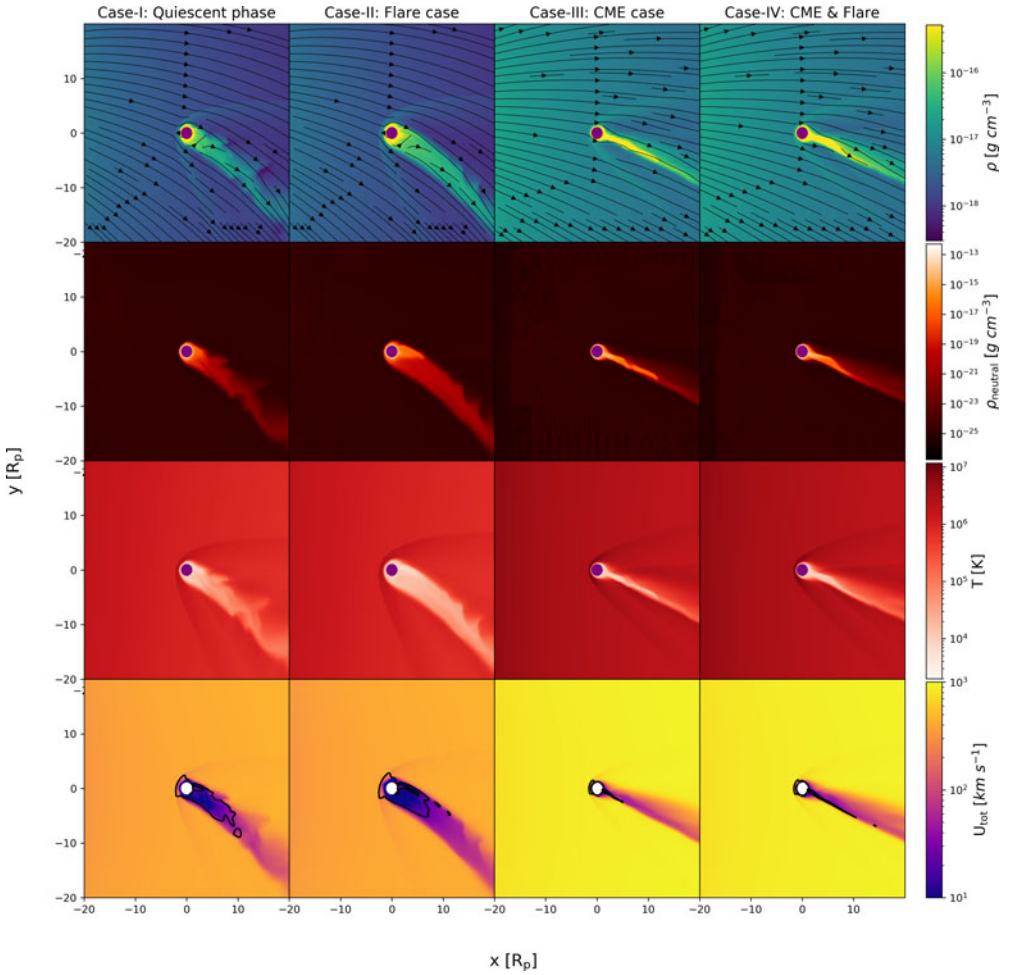

Figure 2. Total density, density of neutral material, temperature and total velocity are shown in first column from top to bottom rows respectively for the quiescent phase. Second, third and fourth columns show same quantity as first column but for a flare case, a CME case and for a flare and a CME, respectively. Black streamlines in the first row show velocity. The black contour in the bottom row show sonic surface for different cases.

streamlines. As it is clear from total density plot, the stellar wind pushes the day-side planetary material in a tail like structure. The atmospheric escape rate from the planet is 7.6×10^{10} g s^{-1}, which is 27% higher than the escape rate of planetary outflow without stellar wind (Section 2).

3.2. *Case-II: flare case*

For the flare case, we have considered the flare event that happened 8 hours before the transit event in september 2011 for HD189733A (Lecavelier des Etangs et al. 2012). The observed peak X-ray flux during the flaring event is 1.3×10^{-12} erg cm^{-2} s^{-1}, which gives an XUV radiation of $F_{xuv} = 1.5 \times 10^5$ erg cm^{-2} s^{-1}. The stellar wind parameters are same as Case-I. The fundamental properties total density, neutral density, temperature and total velocity of planetary materials in this case is shown in the second column of figure 2. The enhanced XUV radiation due to the flare lifts up more planetary material

https://doi.org/10.1017/S1743921322004963 Published online by Cambridge University Press

and ionises more neutral material than quiescent phase leading higher atmospheric escape rate. The atmospheric escape rate is this case is 1.0×10^{11} g s^{-1}

3.3. *Case-III: CME only case*

We model CME as a dense and faster stellar wind. To simulate a reasonable CME, we have assumed a density of 2.1×10^{-17} g cm^{-3} and a speed of 755 km s^{-1}, which are a factor of 4 and 2.4 larger than the quiescent stellar wind respectively. The temperature of the CME is 5.4×10^4 K. Since we do not consider a flare in this case, XUV radiation is taken same as quiescent phase of the star.

As CME is much faster and denser than stellar, the ram pressure associated with CME is stronger too. As a result, when the CME interacts with planetary atmosphere it totally confines the day side planetary outflow. This is clearly seen in the column 3 of figure 2. In the CME case, the planetary tail is more inclined towards the line joining star and planet compared to the stellar wind case. This is because the planetary tail follows the resultant CME velocity direction after its get affected by the orbital motion of the planet and as CME is faster than stellar wind, the tail gets less affected. The atmospheric escape rate in this case is 3.2×10^{11} g s^{-1}, which 5.3 times higher than planetary outflow only (Section 2).

3.4. *Case-IV: CME and flare*

In this case, we consider a scenario where a flare is followed by a CME directing towards the planet. The XUV radiation is assumed to be same as flare case (Case-II) and the CME properties are taken same as Case-III. The overall planetary atmospheric behaviour (see fourth coumn of figure 2) remains similar as the CME case (Case-III). However, the neutral tail is denser than the CME case only. The atmospheric escape rate is this case 4.0×10^{11} g s^{-1}, which is highest among the all cases considered here.

4. Comparison with transit observation: Ly-α line

We have calculated the synthetic transit spectra for all our four cases to compare with the available Ly-α transit observations for HD189733b. The details of how we calculate synthetic transit spectra is given in Hazra et al. (2022). In figure 3(a), the theoretical transit spectra at mid-transit for all cases including no stellar wind case are shown. The higher transit depths in the high-velocity material show the fact that the stellar CME (Case-III and Case-IV, magenta and orange lines) affects the high-velocity blue-shifted materials in compare to the stellar wind cases (Cases -I and II, blue and green lines).

To compare directly with reported observed values, we convolve our theoretical transit profiles with G140M grating of STIS. In figure 3(b), the convolved lines are shown. The color lines showed the Ly-α absorption after it gets absorbed by the planetary atmospheres in each case we studied here. The out-of-transit Ly-α line is also shown in black for comparison. A zoom in version of the blue wing [(-230) - (-140)] km s^{-1}] and red wing [60-110 km s^{-1}] are shown in figure 3(c) and (d) respectively. Both of the cases, where we include CME (Case-III and IV) show a deeper transit depth but the CME only case (Case-III) shows largest integrated blue wing absorption of 5.1%. Although CME case produces larger transit depth in the blue wing among all the model we considered here, none of our model is able to explain the large absorption of 14.4 ± 3.6% seen in the blue-wing observation.

https://doi.org/10.1017/S1743921322004963 Published online by Cambridge University Press

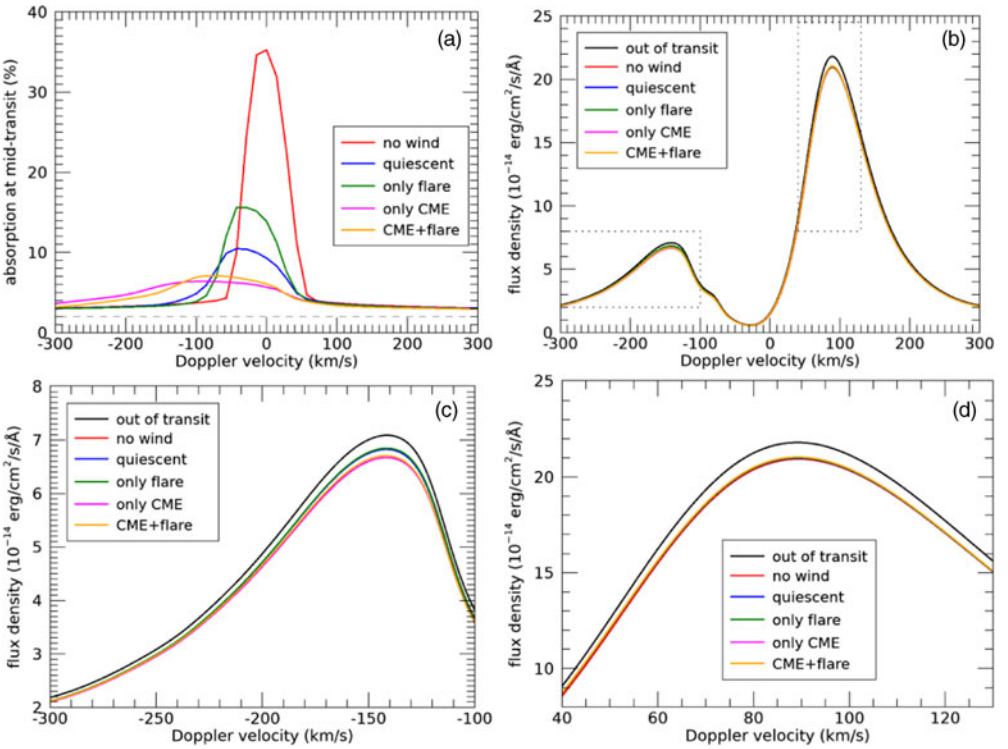

Figure 3. Synthetic Ly-α line profile at mid transit. (a) theoretical line profile; (b) predicted observed profile, convolved with G140M grating mode; (c) same as b, but for the blue wing of the line; (d) same as b, but for the red wing of the line.

5. Conclusions

In this work, we have presented a 3D radiation driven atmospheric escape model and the interaction between radiation driven planetary outflow and stellar transient events. Our model included both neutral and ionised hydrogen (multi-species) and considered photoionisation, collisional ionisation and radiation recombination.

We found that the atmospheric escape rate (mass-loss rate) is higher when we consider CME in our simulations. The CME case with flare enhances the escape rate significantly giving the highest mass-loss rate of 4.0×10^{11} g s^{-1} among all the cases considered here. We also calculated the transit spectra for all cases. We found that the quiescent and flare cases are not able to reproduce the strong absorption in the blue-wing of Ly-α. The CME cases with or without flare (Case-III and Case-IV) show larger absorption of blue-shifted material in compared to the quiescent and flare cases (Case-I and Case-II). Hence, the observed temporal variation seen in blue wing of Ly-α line is more likely to be a consequence of the CME affecting the planetary atmospheres, than the flare changes the energy deposition in the atmospheres of the hot Jupiters.

References

A. Vidal-Madjar, A. Lecavelier des Etangs, J. M. Désert, G. E. Ballester, R. Ferlet, G. Hébrard, and M. Mayor. An extended upper atmosphere around the extrasolar planet HD209458b. *Nature*, 422(6928):143–146, Mar 2003. doi: 10.1038/nature01448.

A. Lecavelier des Etangs, V. Bourrier, P. J. Wheatley, H. Dupuy, D. Ehrenreich, A. Vidal-Madjar, G. Hébrard, G. E. Ballester, J. M. Désert, R. Ferlet, and D. K. Sing. Temporal

https://doi.org/10.1017/S1743921322004963 Published online by Cambridge University Press

variations in the evaporating atmosphere of the exoplanet HD 189733b. *A&A*, 543:L4, July 2012. doi: 10.1051/0004-6361/201219363.

Ruth A. Murray-Clay, Eugene I. Chiang, and Norman Murray. Atmospheric Escape From Hot Jupiters. *ApJ*, 693(1):23–42, Mar 2009. doi: 10.1088/0004-637X/693/1/23.

Gopal Hazra, Aline A. Vidotto, and Carolina Villarreal D'Angelo. Influence of the Sun-like magnetic cycle on exoplanetary atmospheric escape. *MNRAS*, 496(3):4017–4031, August 2020. doi: 10.1093/mnras/staa1815.

S. Carolan, A. A. Vidotto, C. Villarreal D'Angelo, and G. Hazra. Effects of the stellar wind on the Ly α transit of close-in planets. *MNRAS*, 500(3):3382–3393, January 2021. doi: 10.1093/mnras/staa3431.

Gopal Hazra, Aline A. Vidotto, Stephen Carolan, Carolina Villarreal D'Angelo, and Ward Manchester. The impact of coronal mass ejections and flares on the atmosphere of the hot Jupiter HD189733b. *MNRAS*, 509(4):5858–5871, February 2022. doi: 10.1093/mnras/stab3271.

J. Sanz-Forcada, G. Micela, I. Ribas, A. M. T. Pollock, C. Eiroa, A. Velasco, E. Solano, and D. García-Álvarez. Estimation of the XUV radiation onto close planets and their evaporation. *A&A*, 532:A6, Aug 2011. doi: 10.1051/0004-6361/201116594.

John McCann, Ruth A. Murray-Clay, Kaitlin Kratter, and Mark R. Krumholz. Morphology of Hydrodynamic Winds: A Study of Planetary Winds in Stellar Environments. *ApJ*, 873(1):89, March 2019. doi: 10.3847/1538-4357/ab05b8.

M. Salz, S. Czesla, P. C. Schneider, and J. H. M. M. Schmitt. Simulating the escaping atmospheres of hot gas planets in the solar neighborhood. *A&A*, 586:A75, February 2016. doi: 10.1051/0004-6361/201526109.

R. D. Kavanagh, A. A. Vidotto, D. Ó. Fionnagáin, V. Bourrier, R. Fares, M. Jardine, Ch Helling, C. Moutou, J. Llama, and P. J. Wheatley. MOVES - II. Tuning in to the radio environment of HD189733b. *MNRAS*, 485(4):4529–4538, June 2019. doi: 10.1093/mnras/stz655.